Role of the microstructure on the mechanical properties of fully pearlitic eutectoid steels

J. Toribio, B. González, J.C. Matos, F.J. Ayaso
University of Salamanca, Spain
toribio@usal.es

ABSTRACT. This paper analyses how the microstructure of an eutectoid pearlitic steel affects its conventional mechanical properties (obtained by means of a standard tension test) and the associated micromechanisms of fracture. Results show how the yield strength, the ultimate tensile strength (UTS) and the ductility, increase as the continuous cooling rate rises, whereas on the other hand the strain at UTS decreases. The fracture surface exhibits more brittle features when the continuous cooling rate decreases, in such a manner that in the fracture process zone an increasing area appears where the pearlite lamellae can be detected and less regions of microvoids are observed.

KEYWORDS. Pearlitic steel; Heat treatment; Ductility; Fracture surface; Micromechanisms of fracture.

INTRODUCTION

In pearlitic steel, hardness and yield strength increase with decreasing interlamellar spacing following a Hall-Petch type relationship [1-11]. Resistance in pearlite is controlled by processes that occur in the ferrite, the main role of the cementite lamellae (at low stresses) being to limit the slip distance in the ferrite [11]. In contrast, the ductility depends on the prior austenite grain, so that it increases with the decreasing size of such characteristic parameter of the material [12-14].

The high work-hardening rate of pearlite is mainly attributed to the load transferred from the ferrite to the cementite, with a significant contribution due to the effect of the constraint of the hard phase on the ferrite [3]. Steels with thin pearlite and coarse pearlite show similar strain hardening coefficients [15].

The coarse pearlite is deformed in a non-homogeneous way, presenting localized plastic strain in narrow slip bands, while thin pearlite shows a much more uniform strain distribution [13, 15, 16]. In pearlitic steel, plastic strain induces compressive residual stresses in the ferrite and tensile stresses in the cementite, so that the residual stress level is higher in steel with greater interlamellar spacing [10]. Fracture in standard tensile test is determined by processes in the colonies having pearlite lamellae parallel to the tensile axis, where the deformation occurs in narrow bands of locally intense shear stress [11].

This paper studies the influence of pearlitic steel's microstructure on conventional mechanical properties obtained with the standard tensile test. Moreover, an analysis of the different micro-mechanisms involved in fracture by simple tension of the steels has been carried out.

EXPERIMENTAL PROCEDURE

The material used was steel with eutectoid composition and some alloying elements: 0.789% C, 0.681% Mn, 0.210% Si, 0.010% P, 0.218% Cr and 0.061% V. The steel, previously produced by hot rolling, was subjected to various heat treatments, consisting of heating the material in a furnace at 900°C (above the eutectoid temperature) for 1 hour and then cooling it in the closed furnace (PF); with the furnace partially open (PS); or outside the furnace, in the air, at room temperature (PA).

The microstructure of the material was analyzed by metallographic microscopy and by scanning electron microscopy (SEM), after the metallographic preparation of small samples of steel by mounting, grinding and polishing (up to a mirror finish) and attack with Nital 4% (a mixture of 4 ml of nitric acid with 96 ml of ethanol) for several seconds to reveal the microstructure.

Standard tensile tests (three for each material) were performed by using cylindrical specimens of 11 mm in diameter and 300 mm in length. The crosshead speed was 2 mm/min and an extensometer with a gage length of 50 mm was placed in the central part of the specimens. Finally, the fracture surfaces and longitudinal sections of the fractured specimens (after metallographic preparation and attack with Nital 4%) was observed through SEM.

EXPERIMENTAL RESULTS

Microstructural analysis

Using optical microscopy and scanning electron microscopy, the microstructure of pearlitic steels obtained by various heat treatments (Figs. 1 and 2) was observed. The diameter of the pearlite colony d_C was measured by the intercept method [17], which consists of counting the number of grains intercepted by a straight line drawn at random along the micrograph, considering the line's randomness and the randomness of the metallographic cut by means of statistical methods. The average interlamellar spacing of pearlite s_0 was calculated by the method of the circular line [18], a variant to the linear intercept method, in which a circle of known length is drawn on the photograph, and the number of intersecting pearlite lamellae is counted (also taking into account the randomness).

The transformation temperature, which in continuous cooling is determined by the cooling rate, controls interlamellar spacing. Decreasing the cooling rate (or increasing the cooling time) increases interlamellar spacing and the size of the pearlite colony (Tab. 1). Interlamellar spacing is independent of the prior austenite grain size and the size of the pearlite colony [4].

Mechanical properties

From the load-displacement records, resulting from standard tension tests, the true stress-strain curves σ-ε characteristic of each material have been calculated (Fig. 3). In them the existence of a small plateau is observed, following the linear elastic region (with the same slope for all the curves), whose size increases with the cooling rate used in the heat treatment. The elasto-plastic region shows a quasi-parallel curve for the steels analyzed.

(a)	(b)
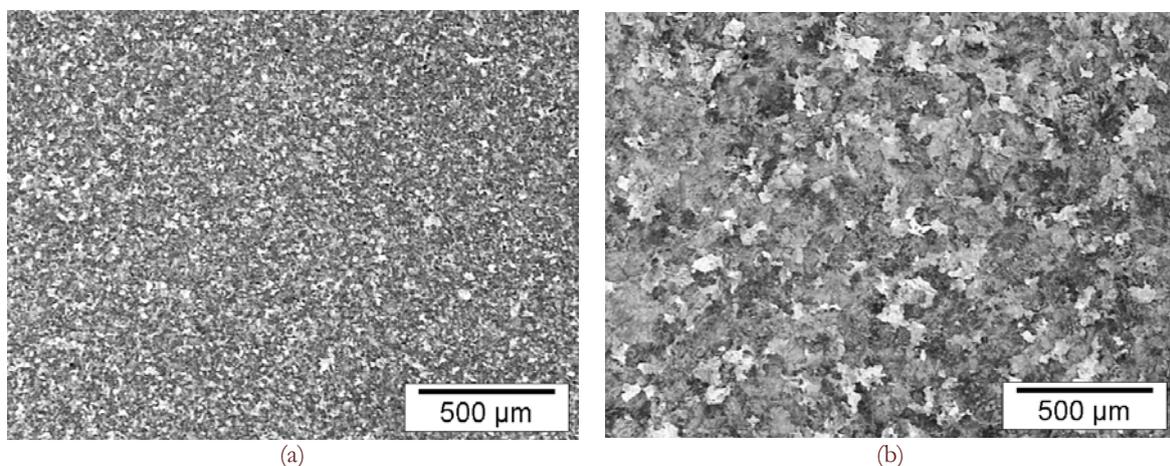
Figure 1: Optical micrographs: (a) air-cooled steel, (b) steel cooled inside the closed furnace.
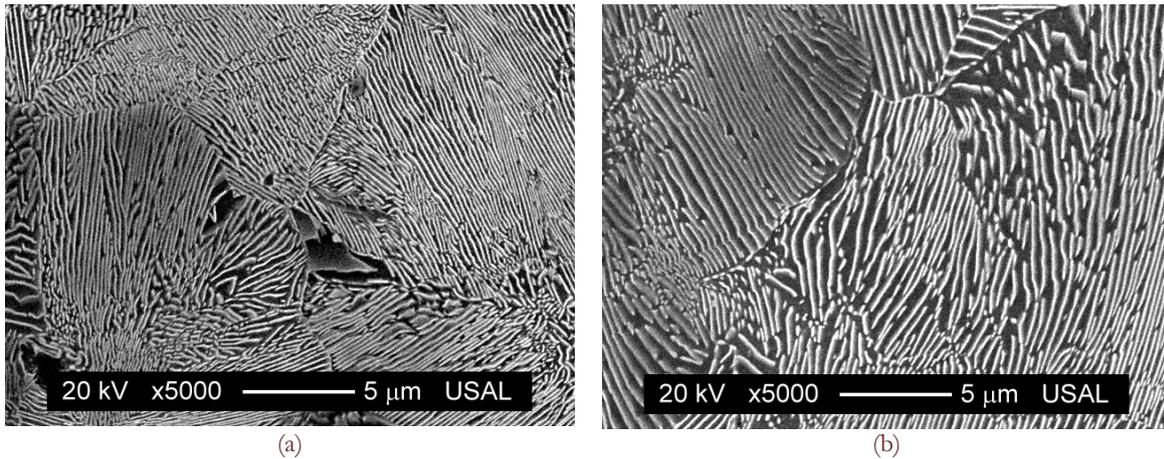
Figure 2: Scanning electron micrographs: (a) air-cooled steel, (b) steel cooled inside the closed furnace.

Steel	PA	PS	PF
d_C (µm)	12	15	19
s_0 (µm)	0.16	0.23	0.26

Table 1: Microstructural parameters.
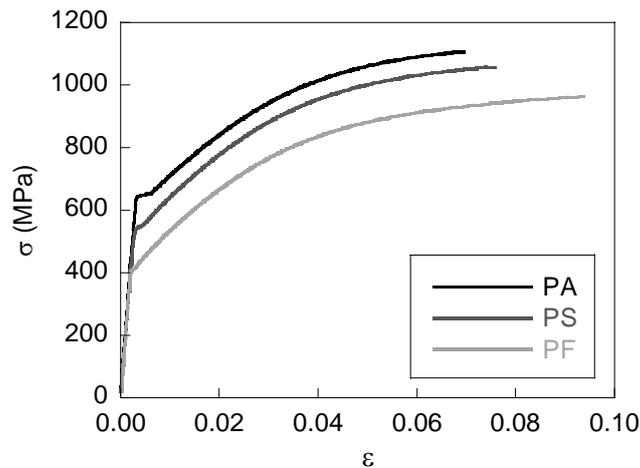
Figure 3: Stress-strain curves (standard tension tests).

The conventional mechanical properties obtained from the standard tension tests are shown in Tab. 2, beside the ductility measured by the reduction in area percentage (*RA*). The three pearlitic steels (PA, PS and PF) have the same Young modulus (*E* ~ 200 GPa), but while the yield strength σ_Y, the ultimate tensile strength (UTS) σ_R and the reduction in area percentage *RA* increase with the increase of the cooling rate used for the thermal treatment of the material, the strain at UTS ε_R decreases.

Steel	E (GPa)	σ_Y (MPa)	σ_R (MPa)	ε_R	RA (%)
PA	202	650	1105	0.067	33
PS	200	560	1055	0.072	20
PF	203	441	965	0.092	14

Table 2: Mechanical properties.

The yield strength in the pearlite is consistent with the stress required to move the dislocations in ferrite between two impenetrable walls made of cementite, where ferrite-cementite interfaces act as barriers to dislocational movement [11]. The stress increases with the refinement of the interlamellar spacing leading to an increase in the resistance, so that the yield strength increases with decreasing interlamellar spacing following a Hall-Petch type relationship [1, 2], with the exponent -1/2. This expression sometimes results in an internal frictional stress in the ferrite with a negative value, which is why some authors prefer to use the exponent -1 in this equation [4, 5, 7].

Increasing the cooling rate, used in the heat treatment of the steel, reduces the maximum uniform elongation attained in standard tension tests, while increasing the total elongation in the necking. Deformation (dislocational structure) has a size effect on interlamellar spacing [15].

Fracture surface

Macroscopically, the steels' fracture surface shows a more brittle appearance with a decreasing cooling rate (Fig. 4). While in the air-cooled steel a necking and cup-cone fracture is observed, steel cooled in the furnace broke without even a necking, and with a more brittle fracture and with a more irregular topography. For steel cooled in the partially-open furnace, the aspect is in between the other two steels analyzed.
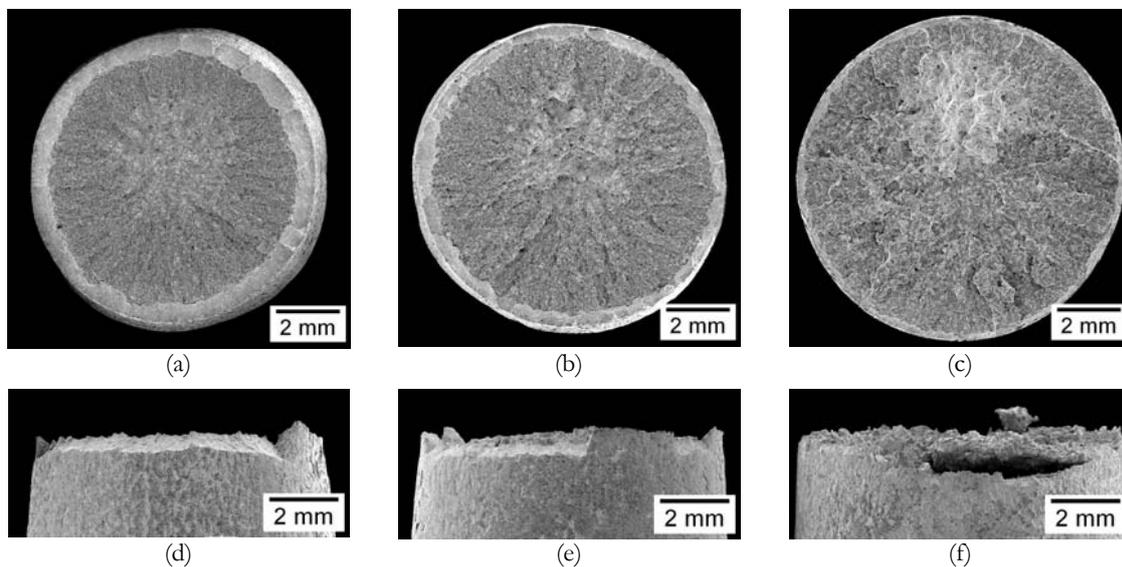
Figure 4: Fracture surfaces of the steels. Top view: (a) PA; (b) PS; (c) PF. Front view: (d) PA; (e) PS; (f) PF.

The fracture begins in the process zone, continues with an unstable propagation zone with a radial form to the wire surface, and ends at the external ring. The fibrous process zone, situated in the central area of the wire (of a lighter color in the photographs), is deviated from the center of the wire; to a greater extent as the cooling rate used in the treatment decreases. The catastrophic propagation zone shows radial micro-cracking, which grows more winding with increasing cooling time, while the external ring thickness decreases (ductile shear lip inclined 45°). The fracture surface's roughness increases with decreasing cooling rate (Fig. 4), and, in some tests, for the steel cooled inside the furnace, secondary cracking contained in the cross section of the wire was also observed (Fig. 4f).

Fractographic analysis

For the air-cooled steel, the process zone at high magnification shows the presence of microvoids (ductile fracture mechanism) of various sizes (round and elongated) along with small regions where pearlite lamellae are observed (Fig. 5a). In steel cooled inside the closed furnace, regions formed by pearlite lamellae are more extensive than in the air-cooled steel, thus presenting a more brittle fractography (Fig. 5b).

In the unstable propagation zone, the fractography consists of cleavage facets, with microvoids regions among them (Fig. 6). For air-cooled steel the size of these cleavage facets (Fig. 6a) is smaller than for steel cooled in the closed furnace (Fig. 6b), a phenomenon related to the size of the prior austenite grain. The microvoid regions between the cleavage facets are most abundant in the air-cooled steel (with more ductile fractography) than in steel cooled inside the furnace.
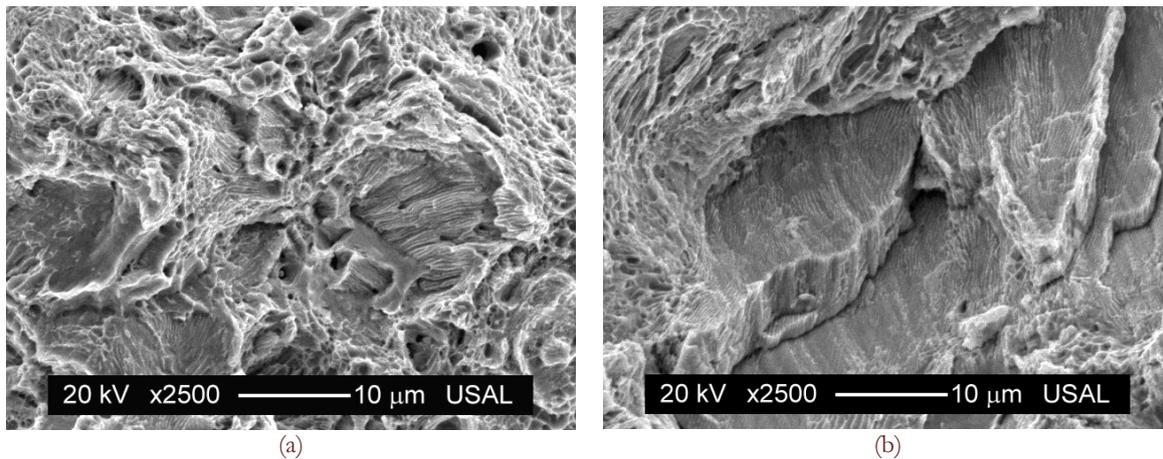
Figure 5: Process zone: (a) air-cooled steel, (b) steel cooled inside the closed furnace.
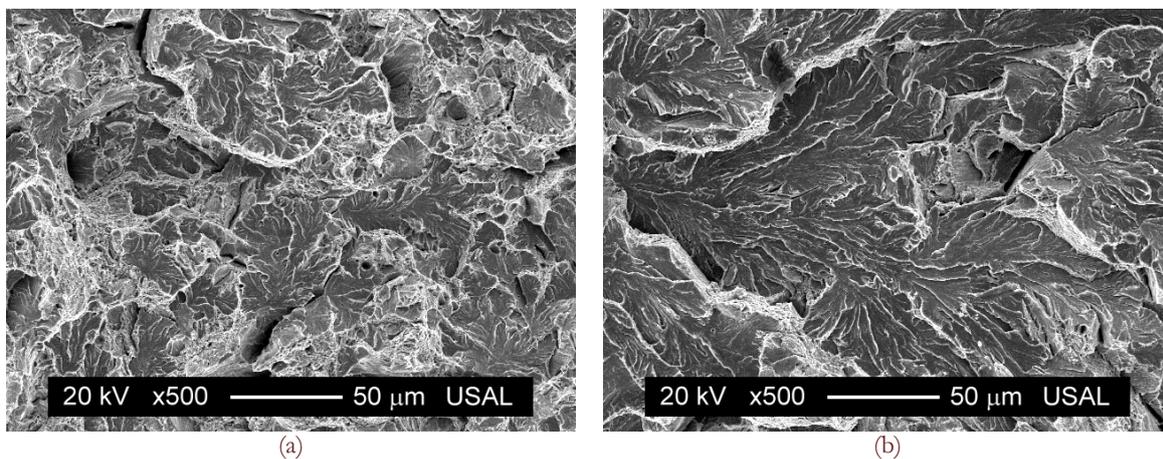
Figure 6: Unstable propagation zone: (a) air-cooled steel, (b) steel cooled inside the closed furnace.

The critical fracture unit has demonstrated to be a region where the ferrite (and cementite) of neighboring colonies share a common orientation {100}. The size of this orientation unit is controlled by the prior austenite grain size and can be calculated by measuring the extension of cleavage facets appearing on the fracture surface [5, 19].

Fracto-metalographic analysis
The specimens' cuts along longitudinal sections allow the observation, in areas close to the fracture surface, of the micro-structural damage that the material has undergone because of the plastic strain occurring during the standard tension test. In many of the colonies whose lamellae have an orientation close to the axial one of the wire (direction in which the load is applied in the standard tension test) the existence of abundant microcracking is observed (Fig. 7). Therefore, the fracture is determined by processes in the pearlite colony with the lamellae being parallel to the tensile axis, where the deformation occurs in narrow bands of locally intense shear stress [11] according to the Miller-Smith mechanism [20]. In this phenomenon the slip bands in the ferrite produce microcracking in the cementite plates, followed by tearing in the ferrite lamellae.
In the colonies with lamellae of thin thickness (air-cooled steel) microcracks with uneven appearance (with regards to the crack opening) and shorter in length than the colony's size are observed (Fig. 7a). On the other hand, the colonies with greater lamellae thickness (steel cooled inside the closed furnace), the inclined cracking is generally of greater length (even across the complete colony) and looks more uniform (Fig. 7b).
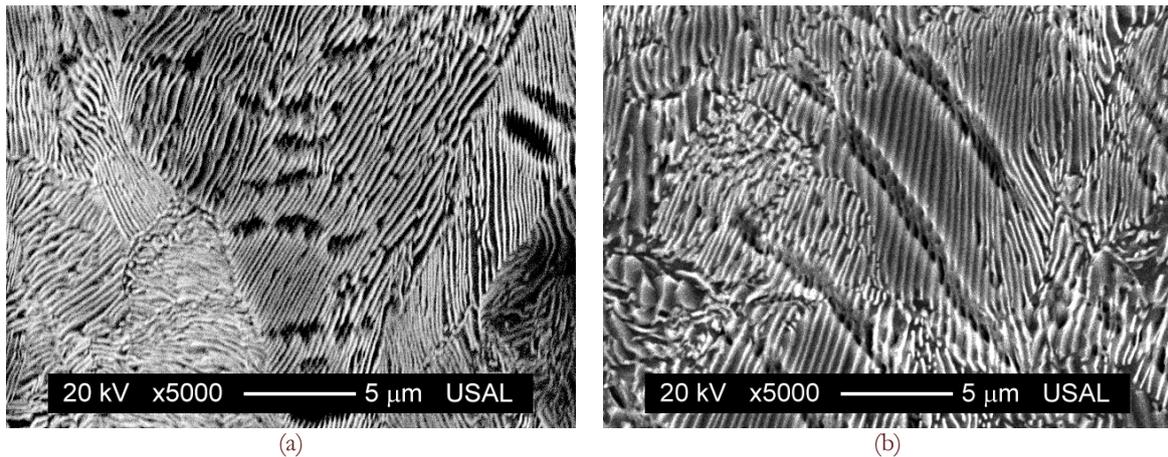
Figure 7: Micro-structural damage near to fracture surface: (a) air-cooled steel, (b) steel cooled inside the closed furnace.

CONCLUSIONS

The following conclusions have been drawn from this work regarding the conventional mechanical properties of pearlitic steel (obtained by standard tension test) and its fracture surface:

(i) The steel's strength (yield strength and ultimate tensile strength) rises with the increase of the cooling rate during thermal treatment.

(ii) Increasing the cooling rate decreases the strain for maximum load (uniform elongation) and increases the reduction in area percentage in the neck (non-uniform elongation).

(iii) Macroscopically, the fracture surface under tension presents a more ductile aspect (with more plastic strain) as the cooling rate increases.

(iv) The process zone fractography (fracture initiation) is formed by mixing two fracture micromechanisms, microvoids and areas where the pearlite lamellae are observed.

(v) As the cooling time increases, in the process zone the surfaces where the ferrite-cementite lamellae are observed increase, while the microvoid zones decrease.

ACKNOWLEDGEMENTS

REFERENCES

[1] Hall, E.O., The deformation and ageing of mild steel: III Discussion of results, Proc. Phys. Soc. Sect., B64 (1951), 747-753.

[2] Petch, N.J., The cleavage strength of polycrystals, J. Iron Steel Inst., 174 (1953) 25-28.

[3] Karlsson, B., Lindén, G., Plastic deformation of eutectoid steel with different cementite morphologies, Mater. Sci Eng., 17 (1975) 153-164.

[4] Marder, A.R., Bramfitt, B.L., The effect of morphology on the strength of pearlite, Metall. Trans., 7A (1976) 365-372.

[5] Hyzak, J.M., Bernstein, I.M., The role of microstructure on the strength and toughness of fully pearlitic steels, Metall. Trans., 7A (1976) 1217-1224.

[6] Kavishe, F.P.L., Baker, T.J., Effect of prior austenite grain size and pearlite interlamellar spacing on strength and fracture toughness of a eutectoid rail steel, Mater. Sci. Tech., 2 (1986) 816-822.

[7] Ray, K.K., Mondal, D. The effect of interlamellar spacing on strength of pearlite in annealed eutectoid and hypoeutectoid plain carbon steels, Acta Metall. Mater., 39 (1991) 2201-2208.

[8] Modi, O.P., Deshmukh, N., Mondal, D.P., Jha, A.K., Yegneswaran, A.H., Khaira, H.K., Effect of interlamellar spacing on the mechanical properties of 0.65% C steel, Mater. Charact., 46 (2001) 347-352.

[9] Elwazri, A.M., Wanjara, P., Yue, S., The effect of microstructural characteristics of pearlite on the mechanical properties of hypereutectoid steel, Mater. Sci. Eng. A, 404 (2005) 91-98.

[10] Yahyaoui, H., Sidhom, H., Braham, C., Baczmanski, A., Effect of interlamellar spacing on the elastoplastic behavior of C70 pearlitic steel: experimental results and self-consistent modeling, Mater. Design, 55 (2014) 888-897.

[11] Dollar, M., Bernstein, I.M., Thompson, A.W., Influence of deformation substructure on flow and fracture of fully pearlitic steel, Acta Metall., 36 (1988) 311-320.

[12] da Fonseca, M.d.G.M., de Almeida, L.H., Gomes, L.C.F.C., Le May, I., Effects of microstructural parameters on the mechanical properties of eutectoid rail steels, Mater. Charact., 39 (1997) 1-14.

[13] Bae, C.M., Nam, W.J., Lee, C.S., Effect of microstructural features on ductility in hypo-eutectoid steels, Scripta Mater., 41 (1999) 605-610.

[14] Lewandowski, J.J., Thompson, A.W., Effects of the prior austenite grain size on the ductility of fully pearlitic eutectoid steel, Metall. Trans., 17A (1986) 461-472.

[15] Izotov, V.I., Pozdnyakov, V.A., Luk'yanenko, E.V., Usanova, O.Yu., Filippov, G.A., Influence of the pearlite fineness on the mechanical properties, deformation behavior, and fracture characteristics of carbon steel, Phys. Metal+ Metallography, 103 (2007) 519-529.

[16] Porter, D.A., Easterling, K.E., Smith, G.D.W., Dynamic studies of the tensile deformation and fracture of pearlite, Acta Metall., 26 (1978) 1405-1422.

[17] Abrams, H., Grain size measurement by the intercept method, Metallography, 4 (1971) 59-78.

[18] Hu, X., Van Houtte, P., Liebeherr, M., Walentek, A., Seefeldt, M., Vandekinderen, H., Modeling work hardening of pearlitic steels by phenomenological and Taylor-type micromechanical models, Acta Mater., 54 (2006) 1029-1040.

[19] Park, Y.J., Bernstein, I.M., The process of crack initiation and effective grain size for cleavage fracture in pearlitic eutectoid steel, Metall. Trans., 10A (1979) 1653-1664.

[20] Miller, L.E., Smith, G.C., Tensile fractures in carbon steels, J. Iron Steel Inst., 208 (1970) 998-1005.